Coarse-Grained Modeling of Mucus Barrier Properties

Pawel Gniewek and Andrzej Kolinski*
Laboratory of Theory of Biopolymers, Faculty of Chemistry, University of Warsaw, Warsaw, Poland

ABSTRACT   We designed a simple coarse-grained model of the glycocalyx layer, or adhesive mucus layer (AML), covered by mucus gel (luminal mucus layer) using a polymer lattice model and stochastic sampling (replica exchange Monte Carlo) for canonical ensemble simulations. We assumed that mucin MUC16 is responsible for the structural properties of the AML. Other mucins that are much smaller in size and less relevant for layer structure formation were not included. We further assumed that the system was in quasi-equilibrium. For systems with surface coverage and concentrations of model mucins mimicking physiological conditions, we determined the equilibrium distribution of inert nanoparticles within the mucus layers using an efficient replica exchange Monte Carlo sampling procedure. The results show that the two mucus layers penetrate each other only marginally, and the bilayer imposes a strong barrier for nanoparticles, with the AML layer playing a crucial role in the mucus barrier.

INTRODUCTION

The epithelial membrane-bound mucus layer protects several animal and human organs. It typically consists of two sublayers: the glycocalyx layer, or adhesive mucus layer (AML), and the luminal mucus layer (LML). The AML is composed of large glycosylated proteins and is attached to the cell membrane in a dynamic fashion. From time to time or when strong friction occurs between tissue layers, these glycoproteins are detached from the membrane. The SEA and EGF domains play a crucial role in this mechanism (1,2). These structures are responsible for a variety of biological functions, including cell signaling and microplicae formation (3). The AML is covered by a mucus gel that forms the LML. The LML is composed of smaller mucins whose properties differ from those of AML mucins (4–7). Mucins are continuously secreted, and therefore the mucus layer has a dynamic character (8,9). Nevertheless, it is reasonable to assume that the system is close to thermodynamic equilibrium. Little is known about the detailed structure and dynamics of mucus on the atomic level. The assumption of quasi-equilibrium makes the problem of determining mucus structure more tractable; however, we have to keep in mind that in reality the motion of nanoparticles in mucus is controlled not only by equilibrium diffusion but also by the steady flow of the gel outward from the cell membrane.

Recently, we described a coarse-grained molecular simulation model of LML (10). The LML mucins (MUC5AC and MUC5B) were represented by flexible chains embedded in the face-centered cubic (fcc) lattice with beads of the chain representing distinct mucin domains (heavily glycosylated domains and hydrophobic, cysteine-rich domains). We designed a simple knowledge-based interaction scheme to

qualitatively mimic the averaged interaction between the mucins' domains. The results show that the system undergoes a sol-gel transition, and that the interactions between the hydrophobic domains and reversible cross-linking between the cysteine-rich domains control the gel fluidity. The picture that emerged from these simulations shows a dynamic network of reversibly cross-linked chains, with a complex topology of the connections.

In this work, we qualitatively expanded the model by adding the membrane-bound AML. The AML is composed of a variety of mucins (MUC1, MUC3A, MUC3B, MUC4, MUC11, MUC12, MUC15, MUC16, MUC17, and MUC20) (3,7). Coating of the cell surface by mucins is responsible for a variety of glycocalyx functions, including surface lubrication, prevention of external body contact with cells, and cell-cell contacts (11). The latter function is especially important in the case of cancer cells, where overexpression of MUC16 is observed (12). MUC16 consists of ~22,000 amino acid residues and is tethered to the outer cell membrane. The domains close to the membrane are weakly hydrophobic, whereas the tail domains are heavily glycosylated and polar. MUC1 and MUC4 are also abundant in the AML, but they are not as glycosylated as MUC16 and are much shorter than MUC16 mucin (<10% and 40% of the MUC16 length, respectively). Thus, it seems that the structural properties of the AML are mainly governed by this long mucin, MUC16 (13).

As noted above, one of the functions of the mucus layer is to prevent the cell surface from contacting nanoparticles of various kinds, including viruses, dust, and combustion residues. Little is known about the specific mechanism of AML action. This is because the AML is inherently bound to the cell surface and thus cannot be easily studied under in vitro conditions. In this work, we studied the penetrability of the mucus layer by small nanoparticles that are chemically inert and interact in a nonspecific fashion with mucins.

Furthermore, we analyzed the effect of the excluded volume, which is entropic in nature.

MATERIALS AND METHODS

LML model

Coarse-grained LML simulations have been described recently (10). Here, we outline the main assumptions of the model design. It is assumed that the LML consists mainly of two mucins (MUC5AC and MUC5B) with similar sequences and properties. LML mucin chains are coarse-grained and represented by flexible chains of 20 beads restricted to the fcc lattice. Each bead represents a mucin domain (MUC5AC or MUC5B). The sequences of the model mucins can be schematically written as SHSHSP$_{12}$HHS, where S denotes a cysteine-rich domain, H is a hydrophobic domain, and P stands for a polar, heavily glycosylated domain. Intra- and interchain interactions are assumed in a form of simple contact potentials for pairs of beads occupying adjacent lattice sites. It is assumed that the polar-polar interactions are nonpreferential, polar-hydrophobic repulsive, and hydrophobic-hydrophobic attractive. We chose the strength of interactions between polar segments to be the same as for a thermal polymer solution, motivated by the strong hydration of glycosylated chains and charge neutralization by small ions (Na$^+$ and K$^+$). Previous studies (14,15) showed that H-H and H-P interactions should be of the same magnitude but of opposite signs. Due to the characteristic redox potential of mucus, allowing for reversible cysteine cross-linking, the strength of the S-S interaction is set to be an order of magnitude smaller than the strength of the covalent disulfide bond. The specific magnitudes of these interactions given below (Table 1) resulted from the compilation of such types of interaction schemes designed for idealistic models of globular proteins (14–16). The interactions are expressed in dimensionless k_BT units, being potentials of mean force, reduced to the reference temperature.

AML model

We designed an AML model using a concept similar to that employed in our earlier study (10). We assume that the AML is composed of mucin MUC16. Other mucins that are less relevant for layer structure formation and are of a much lower content (e.g., MUC1 and MUC4) are not included, but we take their presence into account in an implicit fashion by assuming weaker interactions between MUC16 domains, i.e., all equivalent interactions from bulk mucus are weakened by 50%. Consistent with the previously described coarse-grained representation of the gel layer (LML, composed of mucins MUC5AC and MUC5B), the model of MUC16 is a long chain embedded into the fcc lattice. MUC16 consists of ~22,000 amino acids and its lattice chain is represented by 80 freely connected segments. Thus, the mesoscopic model scaling and the mesoscopic representation of LML and AML are self-consistent. The reduced sequence of MUC16 is MA$_{39}$B$_{40}$, where M represents the transmembrane domain (the membrane is represented as

a flat surface), A stands for the hydrophobic EGF and SEA domains (1,2), and B is the sugar-coated domains (similar in composition and structure to the polar domains of LML mucins). Cell surface coverage by MUC16 is assumed to be equal to ~5%, which is consistent with experimental findings (3). At this point, it is necessary to note that the estimation of surface coverage can only be made in an implicit manner. To our knowledge, no experimental work has directly measured membrane coverage by mucins. Therefore, we estimate the surface coverage by fitting the AML thickness (which itself is ambiguously defined) to the experimental data. At the system equilibration stage, the membrane-tethered M domains are allowed to slide in the hypothetical membrane plane without detaching from it. Afterward, the tethering points become fixed. Consistent with the design of the interaction scheme for LML, and taking into consideration the somewhat weaker hydrophobicity of A with respect to H domains, the interactions between A and B domains are as follows: E(B-B) = 0, E(A-B) = 0.25. The interactions between the B domains, from MUC16. and the other domains of the gel-forming mucins (MUC5AC and MUC5B) are of the same characteristic as for interactions of P in MUC5AC or MUC5B, but weakened by 50% (see Table 1). The A domains rarely contact LML mucins, and their interactions with the P, H, and S domains are less relevant.

Sampling scheme

The simulation box is periodical in the XY direction (with the period of 128 Cartesian units: the fcc chain segment has a length equal to $2^{1/2}$), with the Z = 0 plane representing the membrane surface. In most simulations the numbers of AML and LML chains per the periodic box were set to 409 and 1572, respectively, which corresponds to 5% of surface coverage in AML and 4% of the volume fraction of mucins in the LML gel, which corresponds, for example, to the mucin concentration in lungs (17).

We performed simulations using a replica exchange Monte Carlo (REMC) method and stochastic dynamics of individual chains resulting from a long random series of small (localized) micromodifications of the chain conformations (see Fig. 1). We carried out two series of simulations: one for a pure AML system (five independent simulations) and one for an AML/LML system (10 independent simulations), both with immersed

FIGURE 1 Elementary moves employed in the stochastic dynamics of model mucin chains.

TABLE 1   Interaction scheme for the model domains of LML and AML

	P	H	S	A	B
P	**0.0**	**0.5**	**0.5**	0.25	0.0
H	**0.5**	**−0.5**	**−0.1**	−0.25	0.25
S	**0.5**	**−0.1**	**−2.0**	−0.25	0.25
A	0.25	−0.25	−0.25	−0.25	0.25
B	0.0	0.25	0.25	0.25	0.0

To mimic the covalent character of Cys-Cys interactions, only one S-S contact per S domain was counted during the simulations. The entries in bold are from the previously described LML model.
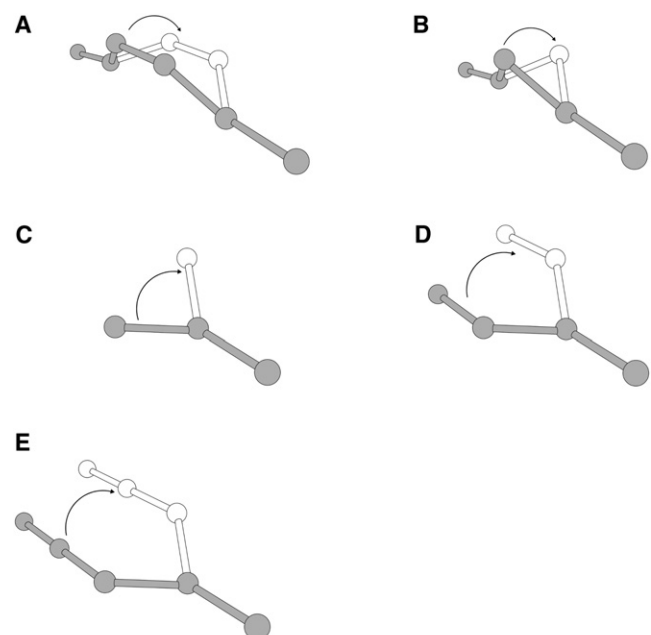
nanoparticles. It is assumed that the surface of an approximately spherical nanoparticle is inert with respect to all mucins, and its diameter is equal to 100 nm. In the lattice model a single nanoparticle is represented as a compact (almost spherical) cluster of 55 lattice vertices, which act on other entities in the system only by means of the excluded-volume interactions. Such a range of nanoparticle size is typical for many problems of transport through gel, including drug delivery problems (18). The motion of nanoparticles was simulated by random moves with the elementary step of one lattice unit. The frequency of various elementary moves of mucin chain fragments and nanoparticles was set to be proportional to the inverse number of the affected segments (1/k for k-segment locally moving mucin chains and 55^{-1} for nanoparticles). REMC simulations were performed for 10 replicas uniformly distributed between T = 0.22 and T = 0.29 (where T is the dimensionless reduced temperature). In the simulations of the sol-gel transition in the LML model (with the same interaction scheme as in the present work), the transition temperature was T = 0.25. The model systems were carefully initiated and equilibrated. First, the model mucins were added successively: ALM mucins attached to the hypothetical membrane and LML mucins in random locations of the MC box satisfying the condition Z > 260 nm. The latter requirement reflects the fact that LML mucins are secreted in a different location of a living tissue and therefore should not be initially entangled with the glycocalyx brush. The starting conformations of AML/LML systems built in such a way were equilibrated (all replicas) for 5×10^4 MC steps. Next, the nanoparticles were successively added at random positions for Z > 1414 nm. This reflects the fact that the nanoparticles come from the outside of the mucus layer. After an additional 2.5×10^4 MC steps, the distribution of nanoparticles converged to an equilibrium. The production run (for separate simulations) included 5×10^5 MC steps for each replica. Ten swaps of randomly selected pairs of adjacent replicas were attempted every 1000 MC steps. Fig. 2 shows a snapshot from simulations of mucus with nanoparticles (100 nanoparticles per MC box correspond to an arbitrarily selected low concentration of ~0.5%).

RESULTS AND DISCUSSION

Determining the range of MUC16 surface density

Due to the enormous complexity of mucus systems, it is very difficult to perform experimental structural studies,

especially under in vivo conditions. Therefore, a straightforward estimation of the surface density of MUC16 chains is not available. However, investigators have made reasonable estimations of the AML thickness (i.e., ~250–300 nm) (17,19). It is known from polymer physics that the thickness of a brush formed by polymers of a given length depends on the surface density of end-tethered chains (20,21). At infinite dilution, a single tethered polymer is a random coil, with dimensions close to Gaussian chains, somewhat depending on the interactions with the surrounding solvent. With increasing surface coverage, the tethered chains expand their dimensions in the direction orthogonal to the surface. Therefore, we performed AML simulations with various surface densities of the tethered MUC16 chains, and the system temperature set to T = 0.25, assumed for the remaining simulations. As expected, with increasing surface density, the distribution of the Z axis component of the end-to-end vector for the MUC16 chains shifted toward larger values (see Fig. 3). The coverage of 0.05 seems be the most reasonable with respect to the experimental data, although this is certainly a qualitative estimation. Of interest, even at twofold-higher surface densities the chains maintain their Gaussian character (distribution of the end-to-end vectors), but the coil shape is highly asymmetric and significantly expanded in comparison with the Gaussian chain model (see Table 2).

The AML alone repels nanoparticles

Fig. 4 shows the equilibrium distribution of the A and B domains of the AML layer and nanoparticles in the absence of the gel LML layer. The glycocalyx imposes a strong
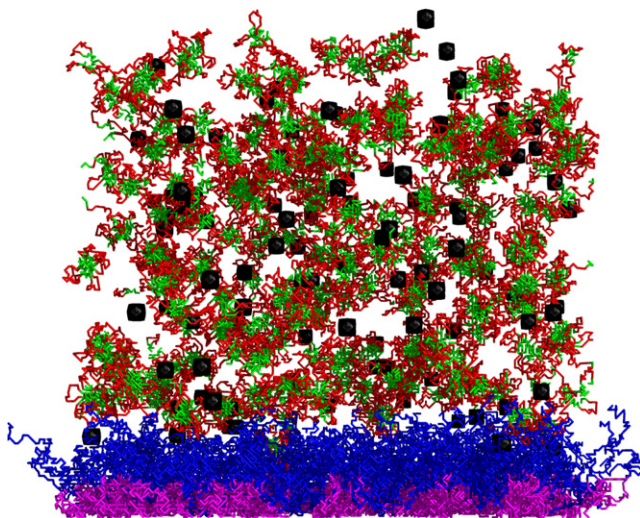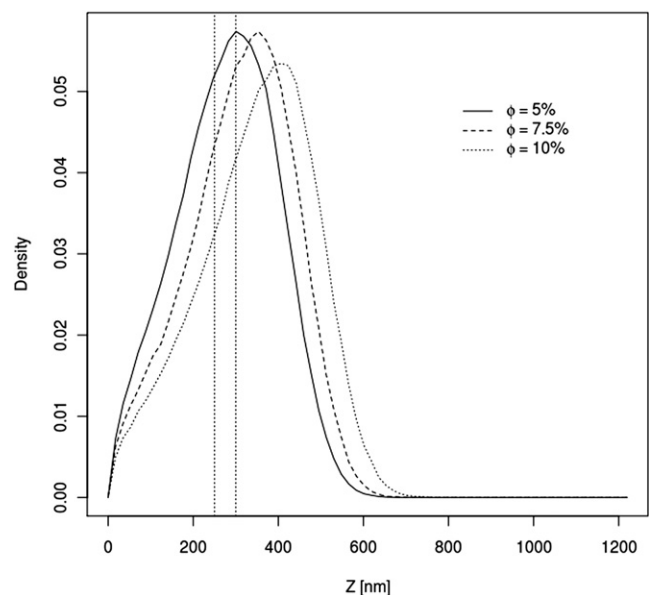

FIGURE 2 Snapshot from REMC simulations of the mucus/nanoparticles system. Black: nanoparticles. Purple and blue: MUC16 A and B domains, respectively. Red and green: polar and hydrophobic domains of LML mucins, respectively.

FIGURE 3 Distributions of the end-to-end vectors of the MUC16 brush for various surface densities of the anchor M domains.

TABLE 2 Mean-square expansion coefficients $\langle S^2/S_0^2 \rangle$ (where S is the radius of gyration) for brush and gel mucin chains as a function of MUC16 surface coverage

Coverage	5.0%	7.5%	10.0%
Brush	3.20	3.44	3.79
Gel	1.75	1.74	1.72

barrier against nanoparticles. The nanoparticle distribution within the layer is of great interest. In the outer polar area of the glycocalyx, the nanoparticle concentration is negligible, regardless of the lower overall density of mucin segments. Near the membrane surface, in the region dominated by hydrophobic A domains, the concentration of nanoparticles increases. Although this effect is not large, it is meaningful, being several times larger than the error of the simulations. This can be easily rationalized. At the temperature of the computational experiment, all segments of the MUC16 chains are highly mobile; however, in the hydrophobic region the mobility is reduced by attractive interactions between the A domains. Therefore, the average distribution of segments is less uniform (in respect to the B dominated region), thus more frequently leaving cavities large enough to acommodate nanoparticles. In contrast, in the B region the chains move faster, and therefore the presence of nanoparticles decreases the system entropy. The value of this entropic barrier can be estimated by means of the potential of mean field theory, and in the case of the presented model is ~2.1–2.5 k_BT. The effect is characteristic for a specific range of mucin surface density. For a sufficiently high density, the size of the free volume becomes
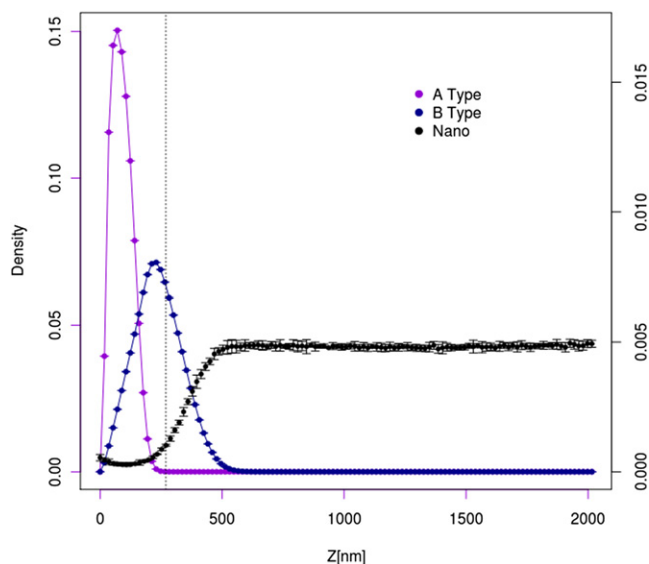
insufficient to accommodate nanoparticles. This is nicely illustrated in Fig. 5, which shows nanoparticle density profiles for different mucin surface concentrations.

Simulations of the AML/LML mucus system

The simulation setup is the same as for the AML system of the lowest surface coverage (surface density of MUC16 f = 5% and T = 0.25), with added LML mucins. The LML mucins penetrate only the lowest-density region of the AML (see Fig. 6) and do not noticeably disturb the AML structure. This is illustrated in Fig. 7, in which the distributions of the densities of the MUC16 B domains in the presence and absence of LML mucins are compared. The distributions are practically indistinguishable. This can be rationalized by considering two facts: First, the density of the LML layer is much lower than the density in the bulk of the AML. Second, the LML mucins form a dynamic network (or micronetworks) due to strong interactions between the cysteine-rich domains, preventing significant interpenetration of the two layers. Finally, the LML layer has no noticeable influence on the equilibrium distribution of nanoparticles (compare Figs. 4 and 6). Thus, the AML layer plays a crucial role as the mucus barrier for inert nanoparticles lacking specific interactions with mucins.

CONCLUSIONS

By performing a coarse-grained REMC simulation of the glycocalyx layer, we were able to estimate the tethering

FIGURE 4 Distribution of A domains (*purple*), B domains (*blue*), and nanoparticles (*black*) for the AML layer (not covered by the gel layer) for the system with surface coverage equal to 0.05. For better readability, the scale for nanoparticle distribution is given at the right-hand side of the plot.
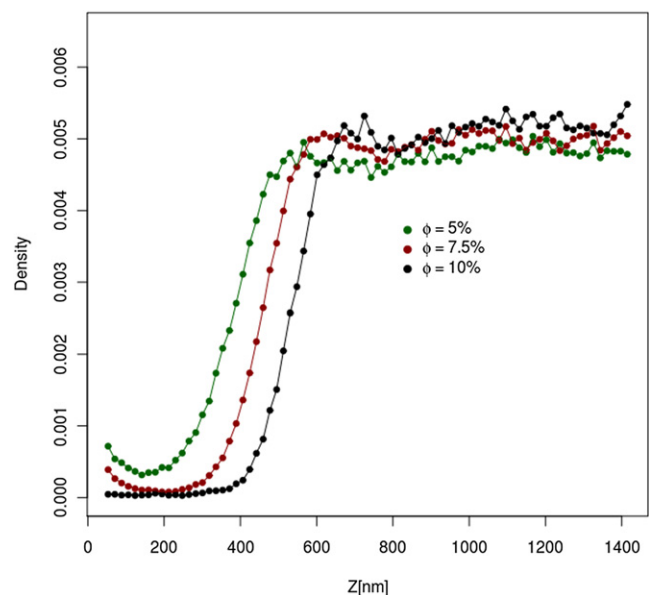

FIGURE 5 Distribution of nanoparticles density for the AML layer (not covered by the gel layer) for various surface coverage. The leftmost points of distributions correspond to nanoparticles. touching the membrane surface.
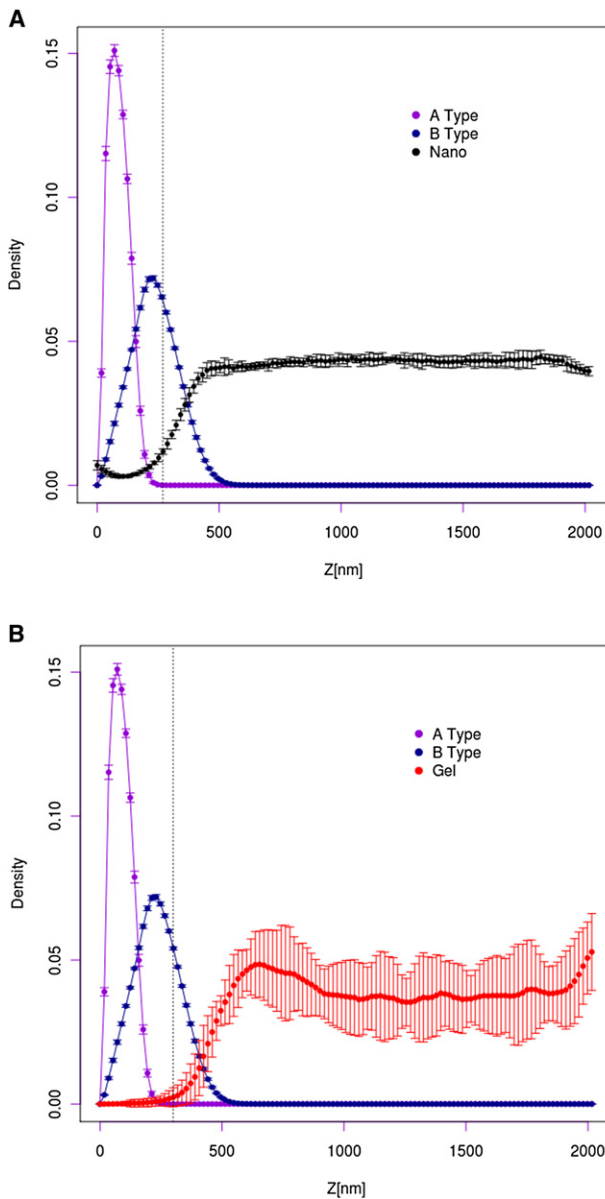
FIGURE 7 Density profiles of the MUC16 B domains in the presence and absence of LML.

FIGURE 6 (*A*) Distribution of MUC16 segments and across the AML/LML mucus layer (for better readability, the scale for nanoparticle distribution is given at the right-hand side of the plot). (*B*) The corresponding distribution of the gel mucins.

density of MUC16 chains and rationalize the experimentally observed thickness of the AML mucus layer. Our results complement the picture of a gel-like mucus that has the character of a dynamic polymer network with complex topology. The results show that at equilibrium (an approximation) the mucus layer is a strong barrier against nanoparticles. The barrier has a topological and entropic nature and does not require any specific particle-mucin interactions. Of interest, the LML layer has very little, if any, effect on the mucus barrier against inert nanoparticles. In agreement with experiments (22), the interface between the two layers is very narrow. This is shown for inert nanoparticles, without
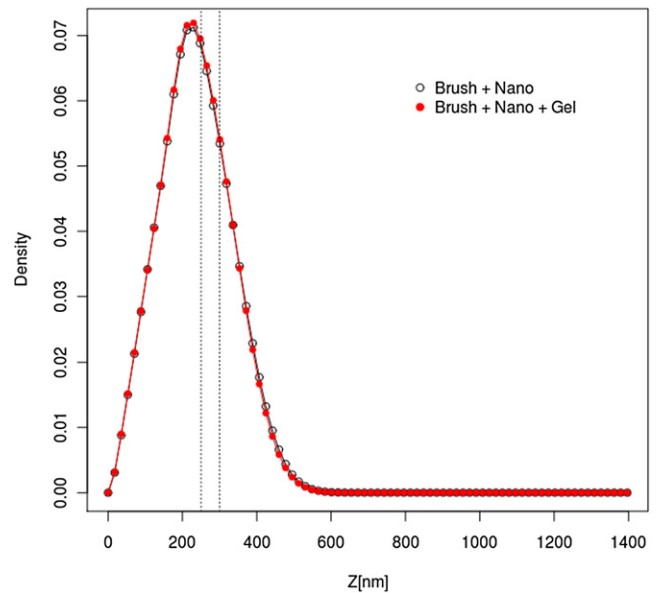
any preferential interactions with LML and AML mucins. We also observed that the presence or absence of the gel layer had no effect on the brush structure. This suggests, in agreement with experimental findings (23), that diffusion in gel can be separated from the transport across the tethered layer.

The approximations assumed in this study impose some restrictions on the resolution of the obtained results. The parameters of the model were chosen to correspond to the existing sparse experimental data (from AML and LML models) and should not be taken as strictly quantitative. Nevertheless, the universality of mucus layers throughout many animal organs, environments, and conditions allows us to conclude that the resulting microscopic picture of the mucus structure and mode of action is qualitatively correct. In the near future we plan to extend the model by treating mucus layers more heterogeneously (i.e., taking into account the subtle difference between mucins), and with a higher resolution (i.e., representing peptide and polycarbonate segments as separate moieties). In future studies we will also try to find model interactions that enable the transport of nanoparticles through mucus layers.

Finally, we note that all-atom molecular-mechanics simulations of such large and highly complex systems remain impractical, whereas simulations of small subsystems and/or short-duration simulations of large systems are possible. Snapshots of equilibrated coarse-grained conformations from the simulations presented in this work could be used as plausible scaffolds for the initiation of all-atom simulations, which otherwise would be impossible due to the lack of experimental structural data.

REFERENCES

1. Govindarajan, B., and I. K. Gipson. 2010. Membrane-tethered mucins have multiple functions on the ocular surface. *Exp. Eye Res.* 90: 655–663.

2. Desseyn, J.-L., D. Tetaert, and V. Gouyer. 2008. Architecture of the large membrane-bound mucins. *Gene* 410:215–222.

3. Gipson, I. K. 2004. Distribution of mucins at the ocular surface. *Exp. Eye Res.* 78:379–388.

4. Thornton, D. J., K. Rousseau, and M. A. McGuckin. 2008. Structure and function of the polymeric mucins in airways mucus. *Annu. Rev. Physiol.* 70:459–486.

5. Lai, S. K., Y. Y. Wang, …, J. Hanes. 2009. Micro- and macrorheology of mucus. *Adv. Drug Deliv. Rev.* 61:86–100.

6. Lai, S. K., Y. Y. Wang, and J. Hanes. 2009. Mucus-penetrating nanoparticles for drug and gene delivery to mucosal tissues. *Adv. Drug Deliv. Rev.* 61:158–171.

7. Hattrup, C. L., and S. J. Gendler. 2008. Structure and function of the cell surface (tethered) mucins. *Annu. Rev. Physiol.* 70:431–457.

8. Verdugo, P., I. Deyrup-Olsen, …, D. Johnson. 1987. Molecular mechanism of mucin secretion: I. The role of intragranular charge shielding. *J. Dent. Res.* 66:506–508.

9. Paz, H. B., A. S. Tisdale, …, I. K. Gipson. 2003. The role of calcium in mucin packaging within goblet cells. *Exp. Eye Res.* 77:69–75.

10. Gniewek, P., and A. Kolinski. 2010. Coarse-grained Monte Carlo simulations of mucus: structure, dynamics, and thermodynamics. *Biophys. J.* 99:3507–3516.

11. Hollingsworth, M. A., and B. J. Swanson. 2004. Mucins in cancer: protection and control of the cell surface. *Nat. Rev. Cancer.* 4:45–60.

12. Blalock, T. D., S. J. Spurr-Michaud, …, I. K. Gipson. 2007. Functions of MUC16 in corneal epithelial cells. *Invest. Ophthalmol. Vis. Sci.* 48: 4509–4518.

13. Hori, Y., K. Nishida, …, Y. Tano. 2008. Differential expression of MUC16 in human oral mucosal epithelium and cultivated epithelial sheets. *Exp. Eye Res.* 87:191–196.

14. Pokarowski, P., K. Droste, and A. Kolinski. 2005. A minimal protein-like lattice model: an α-helix motif. *J. Chem. Phys.* 122:214915–214916.

15. Pokarowski, P., A. Kolinski, and J. Skolnick. 2003. A minimal physically realistic protein-like lattice model: designing an energy landscape that ensures all-or-none folding to a unique native state. *Biophys. J.* 84:1518–1526.

16. Dill, K. A., S. Bromberg, …, H. S. Chan. 1995. Principles of protein folding—a perspective from simple exact models. *Protein Sci.* 4:561–602.

17. Bramwell, M. E., G. Wiseman, and D. M. Shotton. 1986. Electron-microscopic studies of the CA antigen, epitectin. *J. Cell Sci.* 86: 249–261.

18. Cone, R. A. 2009. Barrier properties of mucus. *Adv. Drug Deliv. Rev.* 61:75–85.

19. Nichols, B. A., M. L. Chiappino, and C. R. Dawson. 1985. Demonstration of the mucous layer of the tear film by electron microscopy. *Invest. Ophthalmol. Vis. Sci.* 26:464–473.

20. Murat, M., and G. S. Grest. 1989. Structure of a grafted polymer brush: a molecular dynamics simulation. *Macromolecules.* 22:4054–4059.

21. Lai, P.-Y., and K. Binder. 1992. Structure and dynamics of polymer brushes near the θ point: a Monte Carlo simulation. *J. Chem. Phys.* 97:586–595.

22. Johansson, M. E. V., J. M. Larsson, and G. C. Hansson. 2011. The two mucus layers of colon are organized by the MUC2 mucin, whereas the outer layer is a legislator of host-microbial interactions. *Proc. Natl. Acad. Sci. USA.* 108 (*Suppl 1*):4659–4665.

23. Wang, Y.-Y., S. K. Lai, …, J. Hanes. 2011. Mucoadhesive nanoparticles may disrupt the protective human mucus barrier by altering its microstructure. *PLoS ONE* 6:e21547. 10.1371/journal.pone.0021547.